

pubs.acs.org/JCTC Article

# Nonorthogonal Multireference Wave Function Description of Triplet—Triplet Energy Transfer Couplings

Lee M. Thompson,\* Emily M. Kempfer-Robertson, Saptarshi Saha, Saurav Parmar, and Pawel M. Kozlowski\*



Cite This: https://doi.org/10.1021/acs.jctc.3c00898



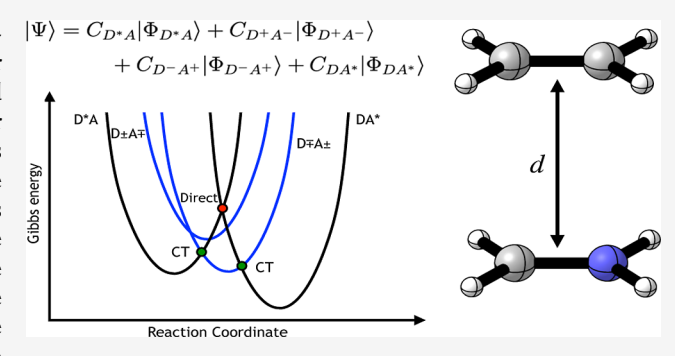
**ACCESS** 

III Metrics & More

Article Recommendations

s Supporting Information

ABSTRACT: In this study, the use of self-consistent field quasi-diabats is investigated for calculation of triplet energy transfer diabatic coupling elements. It is proposed that self-consistent field quasi-diabats are particularly useful for studying energy transfer (EnT) processes because orbital relaxation in response to changes in electron configuration is implicitly built into the model. The conceptual model that is developed allows for the simultaneous evaluation of direct and charge-transfer mechanisms to establish the importance of the different possible EnT mechanisms. The method's performance is evaluated using two model systems: the ethylene dimer and ethylene with the methaniminium cation. While states that mediate the charge-transfer mechanism were found to be



higher in energy than the states involved in the direct mechanism, the coupling elements that control the kinetics were found to be significantly larger in the charge-transfer mechanism. Subsequently, we discuss the advantage of the approach in the context of practical difficulties with the use of established approaches.

## 1. INTRODUCTION

Energy transfer (EnT) involves the exchange of energy between molecules and molecular fragments. A number of EnT mechanisms are possible but are generally divided between Förster EnT,1 which occurs over long distances and is due to the dipole-dipole interaction, and Dexter EnT, which occurs at a shorter range and involves a formal twoelectron transfer between fragments. In the case of triplet energy transfer (TEnT) as well as the two-electron transfer process, there is also a change in the electron spin multiplicity of each fragment in the initial and final states between the singlet and triplet. EnT is of fundamental importance to photophysical processes in chemistry<sup>3-7</sup> and biology<sup>8-12</sup> as well as in materials science. 13-17 However, despite the significance of EnT processes, there is still a lack of fundamental understanding in terms of the mechanism, rate, and theoretical framework. Therefore, in this study, we develop and analyze a new theoretical model of TEnT processes utilizing a nonorthogonal description of diabatic wave functions.

Several approaches have been reported in the literature as to how TEnT rates can be computed. One of the main challenges of computing TEnT rates is the diabatic coupling element, which requires the wave function to be expressed in the diabatic basis, with orbitals localized to different molecules or fragments. The local nature of diabatic orbitals results from the requirement for the invariant character of diabatic states along

the reaction coordinate. One approach for expressing such invariance is configurational uniformity, in which the molecular orbitals (MOs) are chosen such that changes in the configuration interaction (CI) coefficients are minimized along the reaction coordinate. The resulting MOs have the property of MO uniformity, where they exhibit minimal change along the reaction coordinate. 18-20 Use of the diabatic basis is a challenge because computational models for computing the wave function are generally constructed in the adiabatic framework, and so it is not straightforward to change the representation. To address this issue, several computational models have been developed. The two-state model uses localized self-consistent field (SCF) solutions to describe the initial and final states from which the frontier orbitals can be taken to compute the exchange integral, which approximates the diabatic coupling element. 21 In a similar fashion, configuration interaction singles (CIS) can also be used to compute the energy of the lowest triplet states, which can be approximately equated to the same exchange integral that describes the diabatic coupling element.<sup>21</sup> The CIS approach

Received: August 15, 2023



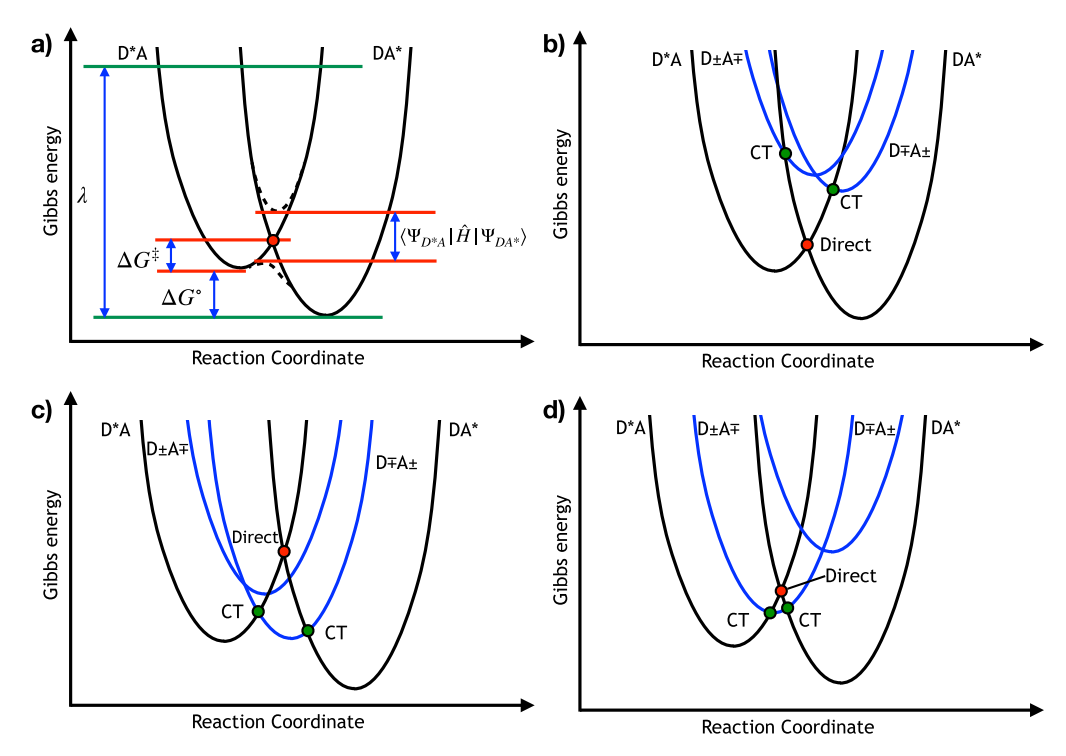


Figure 1. Schematic representation of coupling between diabatic potential energy surfaces used for determination of the rate constant according to the Marcus theory. (a) Pictorial definition of the Gibbs activation energy  $\Delta G^{\ddagger}$ , solvent reorganization energy  $\lambda$ , Gibbs reaction energy  $\Delta G^{\circ}$ , and diabatic electron coupling  $\langle \Psi_D | \hat{H} | \Psi_A \rangle$ . (b) Four-state model showing the case in which direct coupling outcompetes both CT pathways. (c) Four-state model showing the case in which CT coupling outcompetes the direct pathway. (d) Four-state model showing the case in which both CT and direct pathways are competitive.

was subsequently extended using natural localized molecular orbitals,<sup>22</sup> while another approximation is to use the overlap of the triplet frontier orbitals to approximate the relevant exchange integral.<sup>23</sup> Another approach is the fragment spin difference method,<sup>24</sup> in which the difference of spin densities between two states integrated over donor and acceptor fragments is used to evaluate the diabatic coupling element. Rather than approximating the diabatic couplings from adiabatic calculations, alternatively, the diabatic basis can be accessed directly, although it is often not clear how to do so in practice. The constrained density functional theory CI model restricts the properties (number of electrons or spin multiplicity) of a user-defined fragment to directly optimize diabatic wave functions that can then be coupled together through matrix element evaluation, 25 although significant errors in the coupling can result from unreliable spatial constraints, 26 which can be resolved through an orbital-space constrained blocklocalization approach.<sup>27</sup> Finally, the diabatic coupling element can be evaluated using complete active space (CAS) multireference models,<sup>28</sup> but the CAS approach has a number of challenges as we will discuss later.

In this contribution, we outline the use of SCF quasi-diabats for the computation of TEnT diabatic coupling elements. While the diabatic nature of SCF solutions has been commented on previously, in practice, it was challenging to optimize the relevant wave functions due to variational collapse. Recently, there has been a significant number of developments in local SCF optimization, which have enabled straightforward procedures for determining a quasi-diabatic basis.<sup>29–35</sup> In concert with these developments, advancements

in evaluation of nonorthogonal CI matrix elements have provided an opportunity for new approaches for evaluating TEnT diabatic coupling elements. To build a model for TEnT in a nonorthogonal framework, it is necessary to establish the correct protocol and develop an understanding of how the computational approach connects with the underlying physics of the problem. First, we describe the conceptual model of how TEnT rate constants are computed and the relevant parameters that must be included in a model for their evaluation. In particular, we emphasize the role of charge transfer (CT) states that have not previously been properly included in a holistic picture where sequential and direct EnT mechanisms have been treated on the same level. Subsequently, we introduce the detailed equations for the evaluation of nonorthogonal Hamiltonian matrix elements in the context of the diabatic picture. Having introduced the important features of the model, we provide numerical examples to illustrate the relevant points through two model systems: an ethylene dimer and an ethylene/methaniminium cation. We then emphasize how the model overcomes the challenges associated with using CAS adiabatic approaches for the evaluation of coupling elements before concluding.

#### 2. METHODS

**2.1. Conceptual Model.** Conventionally, the description of the rate of EnT processes is based on the Fermi Golden rule, <sup>36</sup> in which the TEnT rate constant is written as

$$k_{\text{TEnT}} = \frac{2\pi}{\hbar} |\langle \Psi_{\text{D}} | \widehat{H} | \Psi_{\text{A}} \rangle|^2 \rho(E)$$
 (1)

where D represents the donor, A represent the acceptor,  $\langle \Psi_{\rm D} | \hat{H} | \Psi_{\rm A} \rangle$  is the diabatic electronic coupling between donor and acceptor, and  $\rho(E)$  is the density of states per unit energy. The density of states can be considered as depending on the nuclear coordinate, and so Marcus theory is an alternative formulation for the rate constant, usually applied in the context of electron transfer<sup>37</sup>

$$k_{\text{TEnT}} = \frac{2\pi}{\hbar} |\langle \Psi_{\text{D}} | \widehat{H} | \Psi_{\text{A}} \rangle|^2 \frac{1}{\sqrt{4\pi R T \lambda}} \exp \left\{ -\frac{\left(\lambda + \Delta G\right)^{\circ^2}}{4\lambda R T} \right\}$$
 (2)

where  $\lambda$  is the reorganization energy and  $\Delta G^{\circ}$  is the free energy change between donor and acceptor states. The formulation for the Marcus rate equation follows from the assumption that the diabatic states can be described as two parabolas shifted along an overall effective reaction coordinate such that the intersection of the two parabolas required to give the free energy of activation  $\Delta G^{\dagger}$  can be written as a function of  $\lambda$  and  $\Delta G^{\circ}$  (Figure 1a). Additionally, it is assumed that the reaction occurs in the high-temperature regime.

The Marcus model assumes that there are two diabatic states that interact and that the rate of TEnT is defined by the intersection point. In the case of TEnT, the states are those in which the triplet is on the donor (D\*A) or on the acceptor (DA\*). However, an additional two intermediate states with a CT character can be obtained through excited state electron transfer to form a doublet donor and acceptor (Figure 2). The

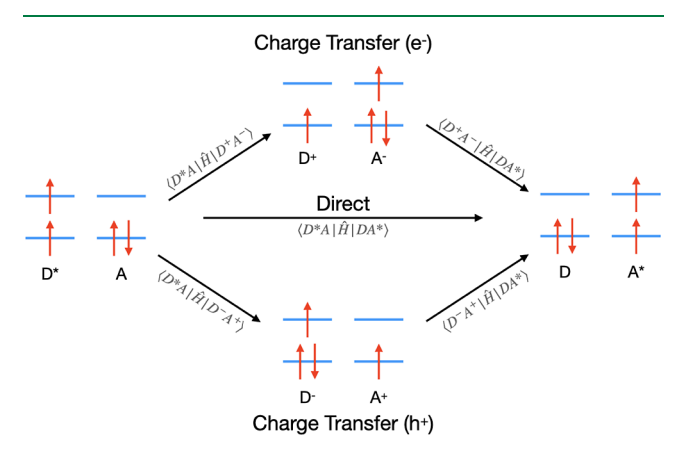


**Figure 2.** Schematic representation of the TEnT demonstrating the interaction pathways linking the exited D\*A to the product DA\*, where the Dexter energy transfer is described by two one-particle couplings and a direct two-particle coupling pathway.

CT states can be formed through either electron transfer from D\*A (D+A-) or hole transfer from D\*A (D-A+). As a result, the overall adiabatic wave function  $|\Psi\rangle$  can be written as a linear combination of the four diabatic states

$$\begin{split} |\Psi\rangle &= C_{\mathrm{D}^*A} |\Phi_{\mathrm{D}^*A}\rangle + C_{\mathrm{D}^+A^-} |\Phi_{\mathrm{D}^+A^-}\rangle + C_{\mathrm{D}^-A^+} |\Phi_{\mathrm{D}^-A^+}\rangle \\ &+ C_{\mathrm{D}A^*} |\Phi_{\mathrm{D}A^*}\rangle \end{split} \tag{3}$$

where  $\{C\}$  are coefficients that mix the diabatic states and  $\{|\Phi\rangle\}$  are the diabatic states. In the four-state model, TEnT can occur either through a direct mechanism, which is formally a double excitation, or sequentially through either the electron or hole CT states, i.e., as two single electron excitations. Extending the Marcus theory to the four-state model, the mechanism that is prevalent depends on the relative energies of the different processes. Although we perform numerical

analysis for isolated systems, the nature of the environment can play an important role in modifying the favorability of different processes, particularly for CT processes that exhibit significant charge separation. Figure 1b shows the case where the direct mechanism outcompetes the CT mechanism, and Figure 1c shows the case in which the CT mechanism is favored over the direct mechanism. Additionally, a third possible case that can occur is the mixed mechanism, where both the direct and the CT mechanisms are competitive (Figure 1d). The exact nature of the mechanism depends not only on the density of states or Gibbs energy of activation,  $\Delta G^{\dagger}$ , but also on the diabatic electronic coupling. In fact, the density of states is often a small contribution, and electronic coupling is the dominant factor as it defines the energy of the adiabatic surface. As a result, as a first approximation, this study examines the rate constants for each process in terms of the electronic coupling only.

**2.2. Theoretical Development.** While the concepts described in the section above are intuitive, a significant challenge is to determine the diabatic basis in which the rate equation is formulated. As described in the Introduction, use of orthogonal determinant expansions is challenging because the methods are constructed on the adiabatic basis. However, it has been commented on by several authors that through studious use of spin symmetry preservation, it is possible to obtain SCF solutions that are quasi-diabatic in nature. 38,39 However, a challenge with the use of single-reference SCF solutions as quasi-diabats is the inability to describe the multireference character in each diabatic state. As a result, a more complete theory can be formulated through a determinantal expansion of each quasi-diabatic SCF solution. While there are a number of ways to achieve such an expansion, including UNOCAS, 40 half-projection 41-43 (or a spin coupled expansion in the case of more than two singleelectron sites<sup>44</sup>), or projection through collective rotation of the electron spin axis,<sup>45,46</sup> in the case of TEnT, the diabatic states are all single determinant in nature owing to their highspin character. Therefore, the use of quasi-diabatic SCF solutions is particularly suitable for determining diabatic electronic coupling in TEnT, especially as they automatically recover electron relaxation in response to the change in electron configuration. Owing to the recent intense interest and development of algorithms for identifying different SCF solutions, it is now possible to more easily identify the relevant quasi-diabatic SCF solutions. 30-35,47,48

Having identified the relevant diabatic SCF solutions, a calculation of the diabatic electron coupling can be performed. However, the calculation is complicated by the fact that the different SCF solutions are generally nonorthogonal. As a result, to determine the diabatic electron coupling, it is necessary to employ nonorthogonal configuration interaction (NOCI) utilizing the generalized Slater—Condon rules. The NOCI eigenvalue is the energy of the adiabatic state shown in eq 3, while the eigenvectors describe the contribution of each diabatic state. For the sake of completeness, the NOCI adiabatic energy is

$$E_{A} = \sum_{\mu\nu} h_{\mu\nu} \gamma_{\mu\nu}^{A} + \frac{1}{2} \sum_{\mu\nu\sigma\lambda} \langle \mu\nu || \sigma\lambda \rangle \Gamma_{\mu\nu\sigma\lambda}^{A}$$
(4)

in which  $\gamma^{\rm A}_{\mu\nu}$  and  $\Gamma^{\rm A}_{\mu\nu\sigma\lambda}$  are the one-electron and two-electron density matrices for adiabatic state A, respectively. The density matrices are obtained as

$$\gamma_{\mu\nu}^{A} = \sum_{IJ} C_{IA}^{*} C_{JA} N_{IJ} \rho_{3\mu\nu}^{IJ}$$
(5)

$$\Gamma^{A}_{\mu\nu\sigma\lambda} = \sum_{IJ} C^{*}_{IA} C_{JA} N_{IJ} \rho^{IJ}_{1\mu\nu} \rho^{IJ}_{2\sigma\lambda}$$
(6)

where  $N_{IJ}$  is the overlap of determinants I and J computed from the determinant of the occupied—occupied (oo) overlap matrix,  $N_{IJ} = \det(^{IJ}\mathbf{M})$ . The oo overlap matrix is computed as

$${}^{IJ}\mathbf{M} = {}^{I}\mathbf{C}_{\text{occ}}^{\dagger} \mathbf{S}^{J}\mathbf{C}_{\text{occ}} \tag{7}$$

where  $C_{\text{occ}}$  is the occupied MO coefficient matrix and S is the atomic orbital overlap matrix. The transition density matrices depend on the number of orbitals that are orthogonal in  $^{\text{IJ}}M$ , which must be separated from the set of nonorthogonal orbitals using singular value decomposition

$$^{IJ}\mathbf{M} = \mathbf{U}^{IJ}\mathbf{\Sigma}\mathbf{V}^{\dagger} \tag{8}$$

where the singular vectors  $\mathbf{U}$  and  $\mathbf{V}$  are used to transform the MOs as  ${}^{\mathbf{I}}\tilde{\mathbf{C}} = {}^{\mathbf{I}}\mathbf{C}\mathbf{U}$  and  ${}^{\mathbf{J}}\tilde{\mathbf{C}} = {}^{\mathbf{J}}\mathbf{C}\mathbf{V}$  and the singular values  $\mathbf{\Sigma}$  give the overlap between the sets of transformed orbitals. The transition density matrices can then be computed using

$$\rho_{1}^{IJ} = \begin{cases} {}^{J}\mathbf{C}^{IJ}\mathbf{M}^{-1I}\mathbf{C} \text{ or } {}^{J}\mathbf{C}^{IJ}\boldsymbol{\Sigma}^{-1I}\mathbf{C} & \text{for } \dim(\ker({}^{IJ}\mathbf{M})) = 0 \\ \sum_{j} {}^{J}\tilde{\mathbf{C}}_{j}^{I}\tilde{\mathbf{C}}_{j}^{\dagger}/\sigma_{jj} & \text{for } \dim(\ker({}^{IJ}\mathbf{M})) = 1 \\ {}^{J}\tilde{\mathbf{C}}_{j}^{I}\tilde{\mathbf{C}}_{j}^{\dagger} & \text{for } \dim(\ker({}^{IJ}\mathbf{M})) = 2 \\ 0 & \text{for } \dim(\ker({}^{IJ}\mathbf{M})) > 2 \end{cases}$$

$$(9)$$

$$\boldsymbol{\rho}_{2}^{IJ} = \begin{cases} \boldsymbol{\rho}_{1}^{IJ} & \text{for dim}(\ker(^{IJ}\mathbf{M})) = 0 \\ {}^{I}\tilde{\mathbf{C}}_{i}^{J}\tilde{\mathbf{C}}_{i}^{\dagger} & \text{for dim}(\ker(^{IJ}\mathbf{M})) \leq 2 \\ 0 & \text{for dim}(\ker(^{IJ}\mathbf{M})) > 2 \end{cases}$$
(10)

$$\rho_{3}^{IJ} = \begin{cases} \rho_{1}^{IJ} & \text{for dim}(\ker(^{IJ}\mathbf{M})) = 0\\ {}^{I}\tilde{\mathbf{C}}_{i}^{J}\tilde{\mathbf{C}}_{i}^{\dagger} & \text{for dim}(\ker(^{IJ}\mathbf{M})) = 1\\ 0 & \text{for dim}(\ker(^{IJ}\mathbf{M})) > 1 \end{cases}$$
(11)

The diabatic electronic coupling element itself is formed from the contraction of the transition density matrices with the Hamiltonian operator

$$H_{IJ} = \widetilde{N}_{IJ} \left\langle I | \widehat{H} | J \right\rangle = \widetilde{N}_{IJ} \left( \left\langle \mathbf{h} \boldsymbol{\rho}_{3} \right\rangle + \frac{1}{2} \left\langle \boldsymbol{\rho}_{1} \mathbf{G} (\boldsymbol{\rho}_{2}) \right\rangle \right) \tag{12}$$

where  $\mathbf{G}(\rho_2)$  is the contraction of two-electron resonance integrals where  $\rho_2$ ,  $\langle \cdots \rangle$  is the trace and  $\tilde{N}_{\mathrm{IJ}}$  is the pseudodeterminant obtained from the product of the nonzero singular values. To obtain the diabatic coupling elements  $V_{\mathrm{IJ}}$ , the nonorthogonality of quasi-diabatic SCF solutions must be accounted for through symmetric orthogonalization of the constructed Hamiltonian matrix, in which the transformation matrix  $\mathbf{X}$  is obtained from

$$\mathbf{X} = \mathbf{U}\mathbf{n}^{-1/2}\mathbf{U}^{\dagger} \tag{13}$$

where n are the eigenvalues and U are the eigenvectors of N. The resulting orthogonalized diabatic states are indicated by a

tilde  $|\tilde{\Phi}\rangle$ . Alternatively, to avoid explicit calculation of the entire Hamiltonian (which is generally a small matrix anyway), it is possible to extract the diabatic coupling term using

$$V_{IJ} = \frac{H_{IJ} - N_{IJ}(H_{II} + H_{JJ})/2}{1 - N_{IJ}^2}$$
(14)

which is based on a two-state model approximation. Regardless of which approach is used, the NOCI framework enables the description of the full four-state model, allowing all pathways to be studied simultaneously.

**2.3. Computational Details.** To illustrate the concepts explored in the previous sections, we examined two model systems. The first model is the ethylene dimer with  $D_{2h}$  symmetry, while the second model system comprises ethylene and the methaniminium cation with a  $C_s$  symmetry, both of which are in a face-to-face arrangement where the diabatic electron coupling was calculated as a function of the intermolecular distance d (Figure 3). The systems were

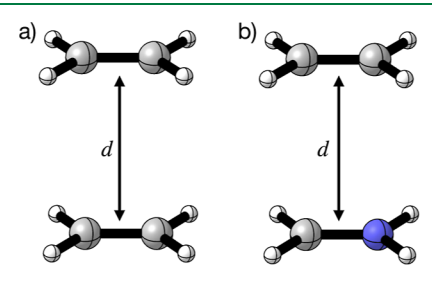


**Figure 3.** Face-to-face arrangement of the ethylene dimer (a) and ethylene/methaniminium cation (b), where d indicates the intermolecular distance.

examined by using monomer separation distances between 3.5 and 5.0 Å with increments of 0.5 Å. The purpose of using these two model systems was to examine the difference between the symmetric and asymmetric donor and acceptor. Similar systems have been considered in the evaluation of other approaches for evaluation of TEnT. The geometries were obtained using Gaussian  $16^{50}$  by optimizing the singlet ground-state geometry with the  $\omega$ B97xD/6-311+G(d) level of theory and constraints on the distance between monomers and point group symmetry. The four quasi-diabatic SCF solutions were then locally optimized using a modified version of Gaussian 16 and then nonorthogonal matrix elements computed with a stand-alone in-house code that utilizes the MQCPack library as well as interfacing with a modified version of Gaussian 16.

# 3. RESULTS AND DISCUSSION

To demonstrate the theoretical protocol described in the Methods section, we applied the method to the calculation of diabatic coupling elements for direct and CT in two model systems. The first model system is the ethylene dimer, which is a symmetric dimer, so hole and electron CT pathways are energetically equivalent. The second model system is ethylene with the methaniminium cation so that the symmetry between hole and electron transfer pathways is removed. Subsequently, we discuss the results in the context of complete active space self-consistent field calculations, followed by diabatization.

**3.1. Ethylene Dimers.** First, the results of the ethylene dimer are discussed. Due to the symmetry of donor and acceptor molecules, the initial and final states (D\*A and DA\*)

are equivalent, and the CT states,  $D^+A^-$  and  $D^-A^+$ , are also equivalent. Computing the diabatic coupling elements allows construction of the Hamiltonian in the basis of the four nonorthogonal diabatic states. Subsequently, symmetric orthogonalization of the nonorthogonal diabatic Hamiltonian yields the basis of orthogonal diabats in which the coupling is correctly expressed. An illustration of the orthogonal diabatic Hamiltonian is shown for the d=3.5 Å geometry (other distances are shown in the Supporting Information)

$$D^*A DA^* D^+A^- D^-A^+$$

$$D^*A \begin{pmatrix} 0.5 & -43.5 & 654.1 & 539.3 \\ -43.5 & 0.0 & -536.9 & -653.5 \\ D^+A^- & 654.1 & -536.9 & 4365.3 & -45.9 \\ D^-A^+ & 539.3 & -653.5 & -45.9 & 4365.6 \end{pmatrix}$$

$$(15)$$

where units are in meV and diagonal elements are shifted by the value of the lowest diagonal matrix element so that the lowest energy diabatic state is at 0.0 meV. Note that small energy differences between states that are equivalent are due to the rounding error in input to the orthogonalization routine. The magnitude of coupling between D\*A and DA\* is significantly smaller than that of coupling involving CT states. The difference in coupling magnitude is consistent with findings from the analysis of singlet fission kinetics, where oneelectron interactions show greater coupling than two-electron interactions.<sup>52</sup> Couplings between diabats of the same type (i.e.,  $D^*A \leftrightarrow DA^*$  or  $D^+A^- \leftrightarrow D^-A^+$ ) involve two-electron transitions, while coupling between diabats of different types involve one-electron transitions. As a result, a qualitative assessment indicates that EnT can occur sequentially through CT states rather than directly as previously considered. An additional point of importance is that the kinetics of the sequential mechanism is controlled by the slowest step (smallest coupling), which in eq 15 is 536.9 meV, compared to the direct mechanism where the coupling is 43.5 meV.

Although based on diabatic coupling elements, the CT pathway is favored over the direct pathway, and the CT states are significantly higher in energy than the two triplets (4365.3 meV). The energy difference is related to the density of states in eq 1 or to Gibbs reaction energy in the exponential term of eq 2. Generally, the pre-exponential term, of which the diabatic coupling element is the main component, is more important than the exponential term, although both terms play a role in the rate. Due to the large energy difference between triplet and CT states, the stepwise CT mechanism may have a small rate constant due to the exponential term, while the direct mechanism has a small rate constant due to the pre-exponential term.

Further analysis of the EnT mechanism can be made through analysis of how the adiabatic states are formed from the diabatic states. The adiabatic states are obtained either through solving the generalized eigenvalue problem for the Hamiltonian in the nonorthogonal diabatic basis or through diagonalization of the Hamiltonian in the orthogonal diabatic basis. The contribution of each orthogonal diabatic basis to each adiabatic state is

$$\begin{split} |\Psi_{T_{l}}\rangle &= +0.68 |\widetilde{\Phi}_{D^{*}A}\rangle - 0.68 |\widetilde{\Phi}_{DA^{*}}\rangle - 0.18 |\widetilde{\Phi}_{D^{+}A^{-}}\rangle \\ &- 0.18 |\widetilde{\Phi}_{D^{-}A^{+}}\rangle \qquad E_{T_{l}} = 0.000 \text{eV} \end{split} \tag{16}$$

$$\begin{split} |\Psi_{\mathrm{T_2}}\rangle &= +0.71 |\widetilde{\Phi}_{\mathrm{D^*A}}\rangle + 0.71 |\widetilde{\Phi}_{\mathrm{DA^*}}\rangle - 0.02 |\widetilde{\Phi}_{\mathrm{D^*A^-}}\rangle \\ &+ 0.02 |\widetilde{\Phi}_{\mathrm{D^-A^+}}\rangle \qquad E_{\mathrm{T_2}} &= 0.312 \mathrm{eV} \end{split} \tag{17}$$

$$\begin{split} |\Psi_{\mathrm{T_3}}\rangle &= -0.02 |\widetilde{\Phi}_{\mathrm{D^*A}}\rangle - 0.02 |\widetilde{\Phi}_{\mathrm{DA^*}}\rangle - 0.71 |\widetilde{\Phi}_{\mathrm{D^*A^-}}\rangle \\ &+ 0.71 |\widetilde{\Phi}_{\mathrm{D^-A^+}}\rangle \qquad E_{\mathrm{T_3}} = 4.148 \mathrm{eV} \end{split} \tag{18}$$

$$\begin{split} |\Psi_{\mathrm{T}_{4}}\rangle &= +0.18|\widetilde{\Phi}_{\mathrm{D}^{*}\mathrm{A}}\rangle - 0.18|\widetilde{\Phi}_{\mathrm{D}^{4}}\rangle - 0.68|\widetilde{\Phi}_{\mathrm{D}^{+}\mathrm{A}^{-}}\rangle \\ &- 0.68|\widetilde{\Phi}_{\mathrm{D}^{-}\mathrm{A}^{+}}\rangle \qquad E_{\mathrm{T}_{4}} = 4.895\mathrm{eV} \end{split} \tag{19}$$

where it can be seen that the lowest two adiabatic states are of a triplet character, while the two highest energy adiabatic states are of a CT character. For each type of adiabatic state, one of the states has leading coefficients with the same sign, while the other state has leading coefficients with the opposite sign. Although this feature is reminiscent of spin adaption, the determinants considered here are high spin; therefore, there is no spin-symmetry adaption required. However, the diabats break spatial symmetry, and so the signs correspond to restoration of the spatial symmetry in the adiabatic picture, in which one adiabat corresponds to the in-phase interaction and the other adiabat corresponds to the out-of-phase interaction, where the signs are dependent on the overlap of the diabats, which are given in the Supporting Information. Although the previous discussion of kinetics was based on the Fermi golden rule in a time-independent formalism, the lowest adiabatic state includes a significant component of a CT character, which illustrates that in reality that there may not be two distinct TEnT mechanisms, but rather the CT acts as resonance states to stabilize the TEnT pathway. 53,54

To understand the role of geometry on TEnT rates, the same analysis as described above was performed at different monomer distances up to 5.0 Å (Table 1 and Figure 4). As is

Table 1. Diabatic Coupling Elements (Absolute Values) in the Ethylene Dimer Calculated as a Function of Monomer Separation Distance Computed by Using Symmetric Orthogonalization

	diabatic coupling elements			
R (Å)	$\langle \mathrm{D*Al}\hat{H} \mathrm{DA*} \rangle$	$\langle \mathrm{D}^*\mathrm{A} \hat{H} \mathrm{D}^*\mathrm{A}^-\rangle$	$\langle \mathrm{D}^*\mathrm{A} \hat{H} \mathrm{I}\mathrm{D}^-\mathrm{A}^+ \rangle$	
3.5	43.5	654.1	539.3	
4.0	26.3	443.2	311.8	
4.5	11.6	292.2	173.0	
5.0	4.7	277.3	75.6	

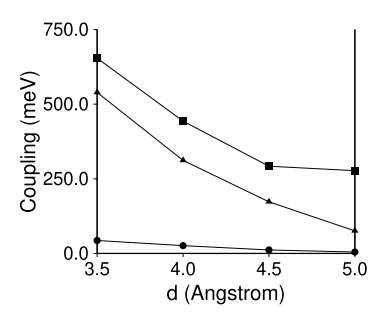


Figure 4. Distance dependence of the ethylene dimer diabatic coupling elements in meV showing the direct coupling (circles), electron CT (squares), and hole CT (triangles).

expected, due to the symmetry of the ethylene dimer system, diabatic coupling elements between D\*A and hole and electron transfer diabats are very similar. The reason that the two values differ by around 100 meV across all geometries is because  $\langle D^*A|\hat{H}|D^+A^-\rangle$  reflects the rate of electron transfer between  $\pi^*$  orbitals, while  $\langle D^*A|\hat{H}|D^-A^+\rangle$  reflects the rate of electron transfer between  $\pi$  orbitals, where the  $\pi^*$  orbital is unoccupied, while the  $\pi$  orbital is already singly occupied. The direct coupling element is much smaller than the CT coupling elements and trends toward zero with distance.

Rather than build and orthogonalize the diabatic Hamiltonian to get the diabatic coupling elements, the coupling between any two diabatic states can be approximated using eq 14, which is the same as forming and orthogonalizing a two-bytwo diabatic Hamiltonian. Thus, the two-state model is an approximation because the diabats are not fully orthogonalized with respect to all of the other diabats. Table 2 shows the

Table 2. Diabatic Coupling Elements (Absolute Values) in the Ethylene Dimer Calculated as a Function of Monomer Separation Distance, Computed Using the Two-State Model (eq 14), Compared to the Direct Coupling (DC) and CIS Results from ref 21

	diabatic coupling elements				ref 21	
R (Å)	$\langle \mathrm{D}^*\mathrm{Al}\hat{H}\mathrm{IDA}^* \rangle$	$\langle D^*A \hat{H} D^+A^-\rangle$	$\langle D^*A \hat{H} D^-A^+\rangle$	DC	CIS	
3.5	98.4	655.5	540.8	99.1	94.2	
4.0	26.2	443.3	311.6	28.5	27.2	
4.5	5.7	292.1	172.2	8.2	8.0	
5.0	1.3	275.7	71.7	2.3	2.2	

results of the two-state model, which are in close agreement for the CT couplings with the full orthogonal results in Table 1, implying that the two-state model works well to avoid finding and building the full diabatic Hamiltonian. However, the direct coupling elements decay more slowly in the fully orthogonal approach than in the two-state model. As a result, the two state model underestimates the role of direct EnT at long distances and overestimates its role at short distances. The two-state model is closely related to previously reported approaches (ref 21), which are found to be in very close agreement with the method presented here. Interestingly, the CIS results, which include both direct coupling and CT coupling, are slightly smaller than the matrix elements only including direct coupling from ref 21, and yet in the current work, the CT matrix elements are an order of magnitude larger than the direct coupling matrix elements, indicating the importance of orbital relaxation in correctly modeling the CT contributions.

**3.2. Ethylene/Methaniminium Cation.** To further illustrate the concepts numerically, we now perform the same analysis as the previous section on the ethylene—methaniminium cation, in which the asymmetry of the dimer causes hole and electron transfer diabats to differ in energy. In fact, the hole transfer pathway, which leads to much higher charge separation than the electron transfer pathway, is shifted so much higher in energy that it can no longer contribute to the kinetics, and so the four-state model can be reduced to a three-state model.

The diabatic coupling elements for the asymmetric system are shown for different intermolecular distances in Table 3 and Figure 5. The general trend is the same as that for the symmetric case, where CT coupling is much larger than direct coupling. However, both mechanisms have smaller diabatic

Table 3. Diabatic Coupling Elements (Absolute Values) in Ethylene and Methaniminium Cations Calculated as a Function of Monomer Separation Distance, Computed Using Symmetric Orthogonalization

	diabatic coupling elements		
R (Å)	$\langle \mathrm{D*Al}\hat{H} \mathrm{DA*}  angle$	$\langle \mathrm{D}^*\mathrm{A} \hat{H} \mathrm{D}^*\mathrm{A}^- angle$	
3.5	5.6	497.1	
4.0	4.3	278.9	
4.5	0.4	158.9	
5.0	1.6	87.8	

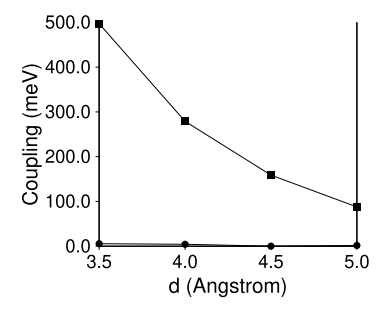


**Figure 5.** Distance dependence of the ethylene/methaniminium diabatic coupling elements in meV showing the direct coupling (circles) and electron CT (squares).

coupling at short distances in the asymmetric system, although the decay is slower so that at 5.0 Å, both the ethylene dimer and ethylene/methaniminium cation have similar magnitude coupling. From 4.5 to 5.0 Å, the direct coupling matrix element increases in value, but this result is an artifact of the small value (1 meV) of the coupling and the accuracy to which diabatic states have been determined. The numerical noise effect is also observed in the diagonal elements of the ethylene dimer Hamiltonian in eq 15, where symmetric diabats differ on the order of 1 meV.

Comparing the orthogonalized diabatic basis three-state model to coupling elements computed from the two-state model (Table 4), the CT couplings are the same for both

Table 4. Diabatic Coupling Elements (Absolute Values) in Ethylene and Methaniminium Cations Calculated as a Function of Monomer Separation Distance, Computed Using the Two-State Model (eq 14), Compared to the Direct Coupling (DC) and CIS Results from ref 21

	diabatic coupling elements		ref 21	
R (Å)	$\langle \mathrm{D*Al}\hat{H} \mathrm{DA*}\rangle$	$\langle D^*A \hat{H} D + A-\rangle$	DC	CIS
3.5	209.3	476.9	212.3	171.4
4.0	60.2	275.0	78.9	56.8
4.5	19.2	158.3	21.2	16.1
5.0	7.6	87.8	5.7	4.5

approaches, as was the case for the ethylene dimer. However, the direct coupling elements are much smaller in the three-state model than in the two-state model. The two-state model only orthogonalizes two diabats at a time. Therefore, the orthogonalized  $|D^*A\rangle$  is different when computing  $\langle D^*A|\hat{H}|D^+A^-\rangle$ , so that there is no consistent orthogonal diabat basis, which leads to overestimation of the direct coupling elements. As in the

ethylene dimer, the two-state direct coupling matrix elements are in agreement with the work of ref 21.

Considering the contribution of diabats to the adiabatic surfaces (see the Supporting Information), it is apparent that the adiabats are of a more mixed character than in the symmetric case. As an example, the lowest adiabatic state at 4.0 Å is

$$|\Psi_{T_i}\rangle = + 0.56|\Phi_{D^*A}\rangle - 0.31|\Phi_{DA^*}\rangle - 0.77|\Phi_{D^*A^-}\rangle$$
 (20)

The largest contribution is of a CT character, but there is a substantial component from triplet diabats. The reason for the mixed character in the asymmetric case is that the CT diabat is much lower in energy and so plays a greater role in the TEnT reaction pathway. As a result, in the three-state orthogonal diabatic basis, the inclusion of the CT state substantially reduces the direct coupling matrix element because the coupling between triplet diabats is mediated through the CT diabat. In contrast, the high energy of the CT state in the symmetric case results in closer diabatic coupling values between the four- and two-state models.

**3.3.** Challenges of Exploring Triplet Energy Transfer Using a CAS Approach. If the nonorthogonal framework is not utilized, the alternative approach is to build diabatic wave functions from a CAS-based wave function expansion, as has been demonstrated in the case of singlet fission. S2 Although, in principle, CAS approaches could provide a good quality assessment of diabatic coupling elements, their practical application has several challenges that can limit their applicability to chemically relevant systems.

The first challenge is the selection of a suitable active space. While active space selection is always a challenge whenever CAS expansions are used, the problem is particularly acute in the case of TEnT. Intuitively, the active space should be four electrons in four orbitals. However, it is not clear how to construct the initial set of orbitals in which expansion is performed. Typically, the initial orbitals for CAS come from a Hartree-Fock (HF) calculation, which is limited to a singleelectron configuration. If the HF electron configuration corresponds to ID\*A), then the orbitals are optimized to describe the triplet on the donor and the singlet on the acceptor. As a result, a simple four-electron four-orbital expansion will not be sufficiently flexible because it cannot account for orbital relaxation that occurs upon excitation to the CT or IDA\* states. To remedy the problem, a larger active space must be selected to describe orbital relaxation, but as the active space is being selected from a set of canonical orbitals, it is difficult to determine if the orbitals being included are correct for describing orbital relaxation in the diabats. Therefore, the solution that is often adopted is to use the largest possible active space so that the chance of including the correct orbitals is maximized, although it is not clear, especially for large systems, if a sufficiently large active space can be chosen within the constraints of computational resources.

The second challenge is how to access CT states, which are considered as an excited state out of the triplet reference. Even if a larger active space can be used, the CT is high in energy compared to the triplet states on the donor or acceptor. As a result, there will be a number of excitations within each monomer that are lower in energy than those of the CT states. Therefore, to try and avoid biasing orbitals to the triplet states, a state average protocol must be used. However, the CAS picture is in terms of adiabatic states, and therefore, it is not

possible to know in advance how to correctly assign weights for state averaging. Alternatively, targeting a single CT state in CAS may cause convergence problems.

The third challenge is to construct the coupling elements on a correctly defined diabatic basis. Assuming that the correct set of canonical orbitals have been identified and the active space is sufficiently large to accommodate orbital relaxation effects, diabatization must be performed and coupling elements must be determined on the diabatic basis. Performing diabatization of the canonical orbitals has been studied over several decades and presents its own challenges, such as how to uniquely define the diabatic basis. Additionally, since the correct set of canonical orbitals in the active space cannot be known until diabatization is performed, an iterative approach is required in which the diabatic basis is examined and used to provide information about the correct set of orbitals in the initial CAS calculation.

The fourth issue is the use of a single set of diabatic orbitals on either the acceptor or donor. While the same issues hold for diabatization in the study of TEnT as in other processes, even if the correct diabatic basis can be obtained, there are still additional issues to resolve. In particular, the best set of diabatic orbitals will be different, depending on the spin state and orbital occupation on each monomer. In TEnT, the donor or acceptor can be singlet, doublet, or triplet, depending on the states in the coupling element being determined. As a result, when evaluating the coupling element in the diabatic basis, it is not possible to use a single spin-adapted electron configuration to describe the bra or the ket because there will be significant contributions from a number of electron configurations, which are describing diabat orbital relaxation in response to change in spin state as well as orbital occupation. For example, in determining the diabatic coupling between  $|D^*A\rangle$  and  $|D^+A^-\rangle$ , even if |D\*A can be considered as a single determinant, the | D<sup>+</sup>A<sup>-</sup>\rangle state will have many contributions from the different possible orbitals into which the electron can be transferred because the diabatic basis was built assuming the spin states and orbital occupancy of ID\*A). As a result, the coupling element is computed as the sum of the contributions from the l D\*A> determinant coupling with the many different electron configurations in the diabatic basis describing the  $|D^+A^-\rangle$  state, and the intuitive description of a single diabat is lost.

To avoid these issues, some promising work has been done using nonorthogonal concepts to allow the best diabatic basis to be selected. The NOCI with multiconfigurational fragment wave functions representing the diabatic state (NOCI-F) approach spatially partitions the wave function and performs a separate CAS calculation on the donor and acceptor. The resulting expansions have different orbitals and so are nonorthogonal. 56,57 The total wave function is then constructed by combining orbitals on each fragment as an antisymmetrized product. As a result, the approach avoids the problem of identifying the correct canonical orbital active space because orbitals are constructed directly in the diabatic basis and so also avoids problems arising from diabatization. However, a remaining challenge is that different orbital occupations and spin states on any fragment are still described by a single set of diabatic orbitals, and so, orbital relaxation effects due to changes in these properties are only accounted for through a large orbital expansion. The large orbital expansion combined with nonorthogonality presents a substantial computational challenge and is most suited to deployment on highly parallel leadership class computing

facilities. Similarly, block-localized molecular orbitals permit strict localization of orbitals to fragments, so defining diabatic states, which can be used to extract direct and CT coupling terms using a multistate energy decomposition analysis. 54,58

#### 4. CONCLUSIONS

In this study, we outline the theoretical concepts behind the use of SCF quasi-diabats for the description of TEnT diabatic coupling elements. First, a conceptual model was introduced, explaining the role of the diabatic coupling elements in the calculation of TEnT rate constants. The importance of the consideration of CT states was emphasized, and an approach for constructing the adiabatic state as the linear combination of four diabatic states was developed (four-state model). It was argued that the four-state model approach was particularly effective because of the different orbitals for different configurations (DODC) approach, in which each diabatic state was constructed using the most suitable set of orbitals, avoiding the requirement for orbital relaxation effects to be recovered through long determinant expansions. Owing to the nonorthogonal framework of DODC approaches, specialized computational approaches are required to construct the effective Hamiltonian and subsequent diabatic coupling element. In particular, the use of symmetric orthogonalization to recover coupling elements from the nonorthogonal effective Hamiltonian was emphasized. The performance of the approach was illustrated using two model systems: an ethylene dimer, in which the donor and acceptor are the same, and ethylene with a methaniminium cation, which breaks the symmetry between the donor and acceptor. The coupling was evaluated as a function of the distance, and while CT states were higher in energy, it was found that the diabatic coupling was stronger for the CT pathway than for the direct pathway. Results from the four-state model were compared to the twostate model that has generally been employed for the study of TEnT. It was found that the CT state couplings were similar in the two models but that the two-state model generally overestimated the direct coupling. In particular, for the asymmetric system, it was found that a two-state model fails because different diabats are obtained for a given diabatic state depending on the particular coupling element being evaluated, and these diabats were different from the diabat in the orthogonal diabatic basis computed in the presence of CT states. As a result, we emphasize the importance of correctly constructing the orthogonal diabatic state in which the coupling elements are determined. Finally, we explore the challenges in the use of orthogonal determinant expansions for the calculation of diabatic coupling elements and highlight recent developments utilizing nonorthogonal determinants.

## ASSOCIATED CONTENT

### Supporting Information

The Supporting Information is available free of charge at https://pubs.acs.org/doi/10.1021/acs.jctc.3c00898.

For each geometry of each molecule, molecular coordinates, nonorthogonal diabatic Hamiltonian matrices, diabatic overlap matrices, orthogonalized diabatic Hamiltonian matrices, adiabatic wave functions and energies, and diabatic two-state coupling matrices (PDF)

#### AUTHOR INFORMATION

# **Corresponding Authors**

Lee M. Thompson – Department of Chemistry, University of Louisville, Louisville, Kentucky 40929, United States;
orcid.org/0000-0003-1485-5934;

Email: lee.thompson.1@louisville.edu

Pawel M. Kozlowski — Department of Chemistry, University of Louisville, Louisville, Kentucky 40929, United States; Email: pawel.kozlowski@louisville.edu

#### **Authors**

Emily M. Kempfer-Robertson – Department of Chemistry, University of Louisville, Louisville, Kentucky 40929, United States

Saptarshi Saha — Department of Chemistry, University of Louisville, Louisville, Kentucky 40929, United States Saurav Parmar — Department of Chemistry, University of

Saurav Parmar – Department of Chemistry, University of Louisville, Louisville, Kentucky 40929, United States

Complete contact information is available at: https://pubs.acs.org/10.1021/acs.jctc.3c00898

#### Notes

The authors declare no competing financial interest.

## ACKNOWLEDGMENTS

This material is based on the work supported by the National Science Foundation under Grant 2144905. Emily M. Kempfer-Robertson acknowledges funding through the Arno Spatola Endowment Fellowship. This work was conducted in part using the resources of the University of Louisville's Research Computing group and the Cardinal Research Cluster.

# **■** REFERENCES

- (1) Förster, T. Zwischenmolekulare energiewanderung und fluoreszenz. *Ann. Phys.* **1948**, 437, 55–75.
- (2) Dexter, D. L. A theory of sensitized luminescence in solids. J. Chem. Phys. 1953, 21, 836–850.
- (3) Tyson, D. S.; Castellano, F. N. Intramolecular singlet and triplet energy transfer in a ruthenium(II) diimine complex containing multiple pyrenyl chromophores. *J. Phys. Chem. A* **1999**, *103*, 10955—10960.
- (4) Murphy, C. B.; Zhang, Y.; Troxler, T.; Ferry, V.; Martin, J. J.; Jones, W. E. Probing Förster and Dexter energy-transfer mechanisms in fluorescent conjugated polymer chemosensors. *J. Phys. Chem. B* **2004**, *108*, 1537–1543.
- (5) Lazarides, T.; Sykes, D.; Faulkner, S.; Barbieri, A.; Ward, M. D. On the mechanism of d-f energy transfer in Ru<sup>II</sup>/Ln<sup>III</sup> and Os<sup>II</sup>/Ln<sup>III</sup> dyads: Dexter-type energy transfer over a distance of 20 Å. *Chem.*—*Eur J.* **2008**, *14*, 9389–9399.
- (6) Daub, M. E.; Jung, H.; Lee, B. J.; Won, J.; Baik, M.-H.; Yoon, T. P. Enantioselective [2 + 2] cycloadditions of cinnamate esters: generalizing Lewis acid catalysis of triplet energy transfer. *J. Am. Chem. Soc.* **2019**, *141*, 9543–9547.
- (7) Kratz, T.; Steinbach, P.; Breitenlechner, S.; Storch, G.; Bannwarth, C.; Bach, T. Photochemical deracemization of chiral alkenes via triplet energy transfer. *J. Am. Chem. Soc.* **2022**, *144*, 10133–10138.
- (8) Ford, W. E.; Rodgers, M. A. J. Reversible triplet-triplet energy transfer within a covalently linked bichromophoric molecule. *J. Phys. Chem.* **1992**, *96*, 2917–2920.
- (9) Young, A.; Frank, H. Energy transfer reactions involving carotenoids: Quenching of chlorophyll fluorescence. *J. Photochem. Photobiol., B* **1996**, *36*, 3–15.
- (10) Gust, D.; Moore, T. A.; Moore, A. L.; Kuciauskas, D.; Liddell, P. A.; Halbert, B. D. Mimicry of carotenoid photoprotection in

- artificial photosynthetic reaction centers: Triplet-triplet energy transfer by a relay mechanism. *J. Photochem. Photobiol., B* **1998**, 43, 209–216.
- (11) Zheng, Q.; Jockusch, S.; Rodríguez-Calero, G. G.; Zhou, Z.; Zhao, H.; Altman, R. B.; Abruña, H. D.; Blanchard, S. C. Intramolecular triplet energy transfer is a general approach to improve organic fluorophore photostability. *Photochem. Photobiol. Sci.* **2016**, 15, 196–203.
- (12) Ho, J.; Kish, E.; Méndez-Hernández, D. D.; WongCarter, K.; Pillai, S.; Kodis, G.; Niklas, J.; Poluektov, O. G.; Gust, D.; Moore, T. A.; Moore, A. L.; Batista, V. S.; Robert, B. Triplet—triplet energy transfer in artificial and natural photosynthetic antennas. *Proc. Natl. Acad. Sci. U.S.A.* **2017**, *114*, E5513—E5521.
- (13) Chen, F.; Chang, S.; He, G.; Pyo, S.; Yang, Y.; Kurotaki, M.; Kido, J. Energy transfer and triplet exciton confinement in polymeric electrophosphorescent devices. *J. Polym. Sci., Part B: Polym. Phys.* **2003**, *41*, 2681–2690.
- (14) Köhler, A.; Bässler, H. What controls triplet exciton transfer in organic semiconductors? *J. Mater. Chem.* **2011**, *21*, 4003–4011.
- (15) Mongin, C.; Garakyaraghi, S.; Razgoniaeva, N.; Zamkov, M.; Castellano, F. N. Direct observation of triplet energy transfer from semiconductor nanocrystals. *Science* **2016**, *351*, 369–372.
- (16) Bender, J. A.; Raulerson, E. K.; Li, X.; Goldzak, T.; Xia, P.; Van Voorhis, T.; Tang, M. L.; Roberts, S. T. Surface states mediate triplet energy transfer in nanocrystal—acene composite systems. *J. Am. Chem. Soc.* 2018, 140, 7543—7553.
- (17) Luo, X.; Lai, R.; Li, Y.; Han, Y.; Liang, G.; Liu, X.; Ding, T.; Wang, J.; Wu, K. Triplet energy transfer from CsPbBr<sub>3</sub> nanocrystals enabled by quantum confinement. *J. Am. Chem. Soc.* **2019**, *141*, 4186–4190.
- (18) Ruedenberg, K.; Atchity, G. J. A quantum chemical determination of diabatic states. *J. Chem. Phys.* **1993**, *99*, 3799–3803.
- (19) Nakamura, H.; Truhlar, D. G. The direct calculation of diabatic states based on configurational uniformity. *J. Chem. Phys.* **2001**, *115*, 10353–10372.
- (20) Song, L.; Gao, J. On the construction of diabatic and adiabatic potential energy surfaces based on ab initio valence bond theory. *J. Phys. Chem. A* **2008**, *112*, 12925–12935.
- (21) You, Z.-Q.; Hsu, C.-P.; Fleming, G. R. Triplet-triplet energy-transfer coupling: Theory and calculation. *J. Chem. Phys.* **2006**, *124*, 044506.
- (22) Skourtis, S. S.; Liu, C.; Antoniou, P.; Virshup, A. M.; Beratan, D. N. Dexter energy transfer pathways. *Proc. Natl. Acad. Sci. U.S.A.* **2016**, *113*, 8115–8120.
- (23) Bai, S.; Zhang, P.; Beratan, D. N. Predicting Dexter energy transfer interactions from molecular orbital overlaps. *J. Phys. Chem. C* **2020**, *124*, 18956–18960.
- (24) You, Z.-Q.; Hsu, C.-P. The fragment spin difference scheme for triplet-triplet energy transfer coupling. *J. Chem. Phys.* **2010**, *133*, 074105.
- (25) Yeganeh, S.; Voorhis, T. V. Triplet excitation energy transfer with constrained density functional theory. *J. Phys. Chem. C* **2010**, 114, 20756–20763.
- (26) Mavros, M. G.; Voorhis, T. V. Communication: CDFT-CI couplings can be unreliable when there is fractional charge transfer. *J. Chem. Phys.* **2015**, *143*, 231102.
- (27) Ren, H.; Provorse, M. R.; Bao, P.; Qu, Z.; Gao, J. Multistate density functional theory for effective diabatic electronic coupling. *J. Phys. Chem. Lett.* **2016**, *7*, 2286–2293.
- (28) Ma, L.; Fang, W.-H.; Shen, L.; Chen, X. Regulatory mechanism and kinetic assessment of energy transfer catalysis mediated by visible light. *ACS Catal.* **2019**, *9*, 3672–3684.
- (29) Gilbert, A. T. B.; Besley, N. A.; Gill, P. M. W. Self-consistent field calculations of excited states using the maximum overlap method (MOM). *J. Phys. Chem. A* **2008**, *112*, 13164–13171.
- (30) Thom, A. J. W.; Head-Gordon, M. Locating multiple self-consistent field solutions: An approach inspired by metadynamics. *Phys. Rev. Lett.* **2008**, *101*, 193001–193004.

ı

- (31) Ye, H.-Z.; Welborn, M.; Ricke, N. D.; Van Voorhis, T. σ-SCF: A direct energy-targeting method to mean-field excited states. *J. Chem. Phys.* **2017**, *147*, 214104–214111.
- (32) Barca, G. M. J.; Gilbert, A. T. B.; Gill, P. M. W. Simple models for difficult electronic excitations. *J. Chem. Theory Comput.* **2018**, *14*, 1501–1509.
- (33) Thompson, L. M. Global elucidation of broken symmetry solutions to the independent particle model through a Lie algebraic approach. *J. Chem. Phys.* **2018**, *149*, 194106.
- (34) Carter-Fenk, K.; Herbert, J. M. State-targeted energy projection: A simple and robust approach to orbital relaxation of non-aufbau self-consistent field solutions. *J. Chem. Theory Comput.* **2020**, *16*, 5067–5082.
- (35) Dong, X.; Mahler, A. D.; Kempfer-Robertson, E. M.; Thompson, L. M. Global elucidation of self-consistent field solution space using basin hopping. *J. Chem. Theory Comput.* **2020**, *16*, 5635–5644.
- (36) Fermi, E. *Nuclear Physics*; University of Chicago Press: Chicago, 1950.
- (37) Subotnik, J. E.; Vura-Weis, J.; Sodt, A. J.; Ratner, M. A. Predicting accurate electronic excitation transfer rates via Marcus theory with Boys or Edmiston-Ruedenberg localized diabatization. *J. Phys. Chem. A* **2010**, *114*, 8665–8675.
- (38) Thom, A. J. W.; Head-Gordon, M. Hartree-Fock solutions as a quasidiabatic basis for nonorthogonal configuration interaction. *J. Chem. Phys.* **2009**, *131*, 124113.
- (39) Thompson, L. M.; Jarrold, C. C.; Hratchian, H. P. Explaining the MoVO4–photoelectron spectrum: Rationalization of geometric and electronic structure. *J. Chem. Phys.* **2017**, *146*, 104301.
- (40) Kempfer-Robertson, E. M.; Mahler, A. D.; Haase, M. N.; Roe, P.; Thompson, L. M. Nonorthogonal active space decomposition of wave functions with multiple correlation mechanisms. *J. Phys. Chem. Lett.* **2022**, *13*, 12041–12048.
- (41) Zhao, R.; Hettich, C. P.; Chen, X.; Gao, J. Minimal-active-space multistate density functional theory for excitation energy involving local and charge transfer states. *npj Comput. Mater.* **2021**, *7*, 148.
- (42) Lu, Y.; Gao, J. Fundamental variable and density representation in multistate DFT for excited states. *J. Chem. Theory Comput.* **2022**, 18, 7403–7411.
- (43) Lu, Y.; Gao, J. Multistate density functional theory of excited states. J. Phys. Chem. Lett. 2022, 13, 7762-7769.
- (44) Karadakov, P. B.; Cooper, D. L.; Duke, B. J.; Li, J. Spin-coupled theory for "N electrons in M orbitals" active spaces. *J. Phys. Chem. A* **2012**, *116*, 7238–7244.
- (45) Scuseria, G. E.; Jiménez-Hoyos, C. A.; Henderson, T. M.; Samanta, K.; Ellis, J. K. Projected quasiparticle theory for molecular electronic structure. *J. Chem. Phys.* **2011**, *135*, 124108.
- (46) Sundstrom, E. J.; Head-Gordon, M. Non-orthogonal configuration interaction for the calculation of multielectron excited states. *J. Chem. Phys.* **2014**, *140*, 114103.
- (47) Kowalski, K.; Jankowski, K. Towards complete solutions to systems of nonlinear equations of many-electron theories. *Phys. Rev. Lett.* **1998**, *81*, 1195–1198.
- (48) Barca, G. M. J.; Gilbert, A. T. B.; Gill, P. M. W. Communication: Hartree-Fock description of excited states of H<sub>2</sub>. *J. Chem. Phys.* **2014**, *141*, 111104.
- (49) Mayer, I. Simple Theorems, Proofs, and Derivations in Quantum Chemistry; Springer: New York, NY, 2003.
- (50) Frisch, M. J.; Trucks, G. W.; Schlegel, H. B.; Scuseria, G. E.; Robb, M. A.; Cheeseman, J. R.; Scalmani, G.; Barone, V.; Petersson, G. A.; Nakatsuji, H.; Li, X.; Caricato, M.; Marenich, A. V.; Bloino, J.; Janesko, B. G.; Gomperts, R.; Mennucci, B.; Hratchian, H. P.; Ortiz, J. V.; Izmaylov, A. F.; Sonnenberg, J. L.; Williams-Young, D.; Ding, F.; Lipparini, F.; Egidi, F.; Goings, J.; Peng, B.; Petrone, A.; Henderson, T.; Ranasinghe, D.; Zakrzewski, V. G.; Gao, J.; Rega, N.; Zheng, G.; Liang, W.; Hada, M.; Ehara, M.; Toyota, K.; Fukuda, R.; Hasegawa, J.; Ishida, M.; Nakajima, T.; Honda, Y.; Kitao, O.; Nakai, H.; Vreven, T.; Throssell, K.; Montgomery, J. A., Jr.; Peralta, J. E.; Ogliaro, F.; Bearpark, M. J.; Heyd, J. J.; Brothers, E. N.; Kudin, K. N.; Staroverov,

- V. N.; Keith, T. A.; Kobayashi, R.; Normand, J.; Raghavachari, K.; Rendell, A. P.; Burant, J. C.; Iyengar, S. S.; Tomasi, J.; Cossi, M.; Millam, J. M.; Klene, M.; Adamo, C.; Cammi, R.; Ochterski, J. W.; Martin, R. L.; Morokuma, K.; Farkas, O.; Foresman, J. B.; Fox, D. J. *Gaussian 16* Revision A.03.; Gaussian Inc: Wallingford CT, 2016.
- (51) Thompson, L. M.; Sheng, X.; Mahler, A.; Mullally, D.; Hratchian, H. P. MQCPack, 2022; Vol. 22, p 6.
- (52) Zeng, T.; Hoffmann, R.; Ananth, N. The low-lying electronic states of pentacene and their roles in singlet fission. *J. Am. Chem. Soc.* **2014**, 136, 5755–5764.
- (53) Chan, W.-L.; Berkelbach, T. C.; Provorse, M. R.; Monahan, N. R.; Tritsch, J. R.; Hybertsen, M. S.; Reichman, D. R.; Gao, J.; Zhu, X.-Y. The quantum coherent mechanism for singlet fission: Experiment and theory. *Acc. Chem. Res.* **2013**, *46*, 1321–1329.
- (54) Hettich, C. P.; Zhang, X.; Kemper, D.; Zhao, R.; Zhou, S.; Lu, Y.; Gao, J.; Zhang, J.; Liu, M. Multistate energy decomposition analysis of molecular excited states. *JACS Au* **2023**, *3*, 1800–1819.
- (55) Shu, Y.; Varga, Z.; Kanchanakungwankul, S.; Zhang, L.; Truhlar, D. G. Diabatic states of molecules. *J. Phys. Chem. A* **2022**, 126, 992–1018.
- (56) Straatsma, T. P.; Broer, R.; Sánchez-Mansilla, A.; Sousa, C.; de Graaf, C. GronOR: Scalable and accelerated nonorthogonal configuration interaction for molecular fragment wave functions. *J. Chem. Theory Comput.* **2022**, *18*, 3549–3565.
- (57) Sánchez-Mansilla, A.; Sousa, C.; Kathir, R. K.; Broer, R.; Straatsma, T. P.; de Graaf, C. On the role of dynamic electron correlation in non-orthogonal configuration interaction with fragments. *Phys. Chem. Chem. Phys.* **2022**, *24*, 11931–11944.
- (58) Zhao, R.; Hettich, C.; Zhang, J.; Liu, M.; Gao, J. Excimer energies. J. Phys. Chem. Lett. 2023, 14, 2917–2926.